IMPROVEMENTS, VERIFICATIONS AND VALIDATIONS OF THE BOW CODE

S.D. YU, M. TAYAL and P.N. SINGH

Atomic Energy of Canada Limited
2251 Speakman Drive, Mississauga, Ontario, Canada L5K 1B2

ABSTRACT

The BOW code calculates the lateral deflections of a fuel element consisting of sheath and pellets, due to temperature gradients, hydraulic drag and gravity. The fuel element is subjected to restraint from endplates, neighboring fuel elements and the pressure tube. Many new features have been added to the BOW code since its original release in 1985. This paper outlines the major improvements made to the code and verification/validation results.

INTRODUCTION

Bowing is defined as the lateral deflection of a fuel element. During irradiation, bowing occurs due to in-service temperature and external loads. Assessments of bowing of fuel elements can help demonstrate the integrity of nuclear fuel and its surrounding components. Figure 1 shows the structure and configuration of a CANDU® 6 fuel bundle.

The computer code BOW may be used to establish limiting conditions for which element deflection is sufficiently low for thermal-hydraulic conditions to be acceptable. BOW can be used to assess element bow under nominal system pressure, high element power, and dryout that lasts for a few seconds (no creep).

The original version of the BOW code [1] calculated deflections in the two lateral directions (horizontal and vertical), and rotations about the same two lateral directions. The code has now been expanded to calculate the local strains, stresses, curvatures, contact forces, change in element length, and critical buckling load. In calculating these quantities, the code accounts for appendages, length differentials among elements in neighbouring rings, initial bow, radial webs of the endplates, contacts with the pressure tube, local dryouts, and non-circular cross-sections.

Following a brief discussion on bowing of nuclear fuel, this paper discusses the major improvements made to the BOW code since its original release. These improvements are in the following areas: buckling, strains, stresses, curvature, contact force, change in length, Fourier series representations of endplate spring constants, length differential among neighbouring rings, cross-coupling effects of endplate restraint and simultaneous solutions, effect of appendages, effect of radial webs, non-circular cross sections, and streamlined input/output. Verifications and validations of the BOW code against independent solutions and experiments are given.

CANDU®: CANada Deuterium Uranium is a registered trademark of AECL.

Presented at the Fourth International Conference on CANDU Fuel, Pembroke, Canada, 1995 October 1-4.

BACKGROUND

Under operating conditions, the neutron–flux gradient causes a temperature gradient in the radial direction. The coolant temperature and sheath–to–coolant heat–transfer coefficient also vary among subchannels between fuel elements, and cause variations in sheath temperature in the circumferential direction at a given axial location. Radial gradients of neutron flux can also cause temperature gradients. The unsymmetric distribution of temperature with respect to the fuel neutral axis results in unsymmetric thermal expansion, and causes the fuel element to bend toward the long side. This thermally induced deflection may be further increased by the axially applied hydraulic drag load. In addition, the formation of a drypatch on the sheath outer surface due to an increase in power, causes a local increase in temperature in the drypatch area, and further increases the deflection of the fuel element. Figure 2 shows a schematic view of a typical fuel element. A more detailed description of bowing of a fuel element is given in [2].

IMPROVEMENTS TO THE BOW CODE

Buckling

Buckling is important in fuel design. If a fuel bundle has inadequate buckling strength, it may jam against the pressure tube, and cause difficulties in its subsequent removal. The BOW code can be used to assess the buckling strength of different CANDU fuel bundles. The improved version of BOW accounts for the effects of element strength, endplate restraint, appendages and lateral spring applied at an axial location between the two endplates.

For a fuel element with an arbitrary number of appendages, endplate restraint, and lateral spring, BOW first calculates the critical buckling load for the fuel element by neglecting the appendages (if any). A scaling factor, derived using the Ritz method [3], is then applied to the calculated critical buckling load, to account for the strengthening effect of the appendages.

Curvature

Curvature determines the degree of bending for a fuel element. The nodal curvatures are calculated at each finite–element node in the horizontal and vertical coordinate planes. The profiles of the two lateral displacements within a finite element are assumed to be parabolic along the axial direction. Since each finite–element node (e.g., node *i*), with the exception of the two end nodes, is connected to two finite elements, the arithmetic average of the curvatures at the node *i*, calculated from finite element *i* and *i+1*, is taken as the curvature at node *i*. The curvatures in the horizontal and vertical planes are also used to calculate strains and change in the fuel–element length.

Strains

Large strains may cause damage to the sheath and lead to the failure of the fuel element. The sheath total strains due to bending, axial hydraulic loading, and thermal loading are calculated using the equations derived from the unsymmetric bending theory in [4] for each finite–element node along the axial direction. The extreme strains (highest and lowest in value) and their locations (radius and angle) at each nodal location are determined by comparing strains at the mesh grid specified by the user in the BOW input file. The mesh is shown schematically in Figure 3.

Stresses

Pure bending and axial deformation are considered when stresses in the sheath are calculated. The upper and lower bounds of normal stress at every finite–element node are determined by comparing the stresses at the mesh grids shown in Figure 3.

Contact Force

When the deflection of a fuel element at a single axial location exceeds the allowed clearance between the fuel–element and the pressure tube, or between fuel elements, contact will occur. The degree of contact largely determines the magnitude of the contact force. BOW monitors deflection at every finite–element node along the direction in which the clearance(s) are specified in the BOW input file.

Contact must have taken place at node i if the nodal forces, calculated using its two neighbouring elements i and $i+1$, are different, provided that there are no other concentrated external forces applied to node i. The difference is the contact force at node i. Since the finite–element technique is used in the BOW code, the nodal forces may be easily obtained once the nodal displacements are available. When other forces, including concentrated load and external springs, are applied to a finite–element node, the contact force at this node must be modified according to the principle of mechanical equilibrium.

The current version of BOW can be used to analyze multiple contacts of a fuel element with its neighbouring fuel elements or pressure tube. If contacts are detected, BOW writes the total number of contacts and contact forces into the standard output file. As a direct application of the contact force calculation, BOW also calculates the restraining forces and moments exerted to the fuel element by the endplates.

Change in Length

The change in fuel–element length due to bending, thermal expansion and axial compression is calculated in the BOW code. BOW writes the net change and each of the three components into the standard output.

The bending component is calculated for each finite element using a parabolic displacement profile. Since the temperature within a fuel element may vary axially, circumferentially and radially, an average temperature is used to calculate the change in fuel element length for each finite element.

Length Differential Among Neighbouring Rings

The length differential between elements located in different neighbouring rings may cause the fuel element in either of the two rings to bend. Since the elastic deformation of endplate due to concentrated force, bending moment, and/or torque diminishes at a fast rate with distance from the location where the forces and moments are applied, only those fuel elements located in the neighbourhood of radial webs bend noticeably due to the length differential. Other fuel elements are essentially not affected by the length differential.

Fourier Series Representations of Endplate Spring Constants

The endplate restraint, or radial and tangential torsional spring constants, is calculated from both straight beam theory and curved beam theory. For typical endplates of CANDU fuel bundles, the straight beam theory is fairly accurate, compared to the curved beam theory. Nevertheless, the implementation of Fourier series representations of endplate spring constants enables the BOW code to be used for endplate dimensions in a wider range. while providing better results than the straight beam theory used in the original version.

The current version of the BOW code uses the previously established criteria to determine whether the straight beam theory or curved beam theory should be used according to the BOW input data. For the curved beam theory, the code uses the Fourier series representations for the two torsional spring constants. Table 1 compares the endplate spring constants for both straight beam theory and curved beam theory applied to a CANDU 6 endplate. The differences in the spring constants between the two theories are very small.

Cross–coupling Effect of Endplate Restraint

The cross–coupling effect of endplate restraint occurs when the endplate torsional spring constants are obtained in the radial and tangential coordinate plane, and the deflections of the fuel element are obtained in the horizontal and vertical coordinate planes. Because the radial and tangential axes may not coincide with the horizontal and vertical directions, and the radial torsional spring constant may not be equal to the tangential torsional spring constant, the deflection of the fuel element in the horizontal direction is interrelated to the deflection in the vertical direction. The cross–coupling effect can be significant. To account for the cross–coupling effects as a result of endplates, appendages, and non–circular cross sections of a fuel element, one option is to solve the deflections simultaneously in the two lateral directions.

To account for the cross–coupling effect of linear springs $K_{i,r}$ and $K_{i,t}$ applied at node i in the radial and tangential directions, and torsional springs $S_{i,r}$ and $S_{i,t}$ applied at node i in the radial and tangential coordinate planes, the following equations of transformation were used to derive the equivalent spring constants (both lateral and torsional) in the (x,y) coordinates from the known spring constants in the (r,t) coordinates:

$$\begin{bmatrix} K_{i,xx} & K_{i,xy} \\ K_{i,yx} & K_{i,yy} \end{bmatrix} = \begin{bmatrix} K_{i,r}\cos^2\theta + K_{i,t}\sin^2\theta & (K_{i,r} - K_{i,t})\sin\theta\cos\theta \\ (K_{i,r} - K_{i,t})\sin\theta\cos\theta & K_{i,r}\sin^2\theta + K_{i,t}\cos^2\theta \end{bmatrix} \tag{1}$$

$$\begin{bmatrix} S_{i,xx} & S_{i,xy} \\ S_{i,yx} & S_{i,yy} \end{bmatrix} = \begin{bmatrix} S_{i,r}\cos^2\theta + S_{i,t}\sin^2\theta & (S_{i,r} - S_{i,t})\sin\theta\cos\theta \\ (S_{i,r} - S_{i,t})\sin\theta\cos\theta & S_{i,r}\sin^2\theta + S_{i,t}\cos^2\theta \end{bmatrix} \tag{2}$$

where θ is the angle between the fuel–element centreline and the horizontal axis.

Equation (1) applies when lateral spring constants are specified in the radial and tangential coordinate planes; Equation (2) applies when torsional spring constants are specified in the radial and tangential coordinate planes. Consideration of the cross–coupling terms in the above equations requires that the deflections in the horizontal and vertical directions be solved simultaneously, rather than independently. Since the deflections in the two lateral directions are solved independently in the original version of the BOW code, the results are accurate only for the fuel element located at 90° or its multiples, with respect to the horizontal axis. Figure 4 shows the maximum deflection of a typical CANDU 6 fuel element due to a radial temperature gradient driven by an element linear power of 66 kW/m, versus angular locations of the fuel element. Compared with the simultaneous solution, the independent solution yields the largest error at 45°, 135°, 225° and 315°, and the lowest (zero) error at 0°, 90°, 180° and 270°.

Since the temperature gradient due to linear power is in the radial direction, the net deflection of the fuel element should also be in the radial direction. Figure 4 shows that the maximum deflection of the fuel element using the modified BOW code is identical in the radial direction and zero in the tangential direction, for angular locations varying from 0° to 360°. This is in agreement with our expectation. Hence, the revised version of BOW gives an accurate deflection for a fuel element at arbitrary angular locations.

Effect of Appendages

Appendages including, bearing pads and spacers, strengthen the fuel element, provided that the weld is strong enough to transfer the deformation and forces during element bowing. The degree of strengthening is dependent on the material properties and dimensions of the appendages (usually including bearing pads and spacers). For CANDU 6 fuel, the appendages will increase the critical buckling loads by less than 1%. However, for fuel elements of small diameter, the effect of appendages on buckling could be larger.

The appendages tend to have a larger impact on bending of the fuel elements. For a typical CANDU 6 fuel element, the bearing pads and spacers reduce bending in the radial direction due to linear power and hydraulic drag load by about 6%. As noted earlier, the appendages tend to have a greater impact on smaller fuel elements used in advanced fuel designs.

Non-circular Cross Section

The BOW code can also be used to analyze the deflections of a fuel element with various geometries of cross sections. The current version can be used to analyze the following geometries: solid and hollow rectangle, and solid and hollow ellipses. This feature was added to test the code against analytical solutions.

Streamlined Input/Output

The input file required to run the BOW code has been streamlined, to simplify the preparation of input data. The capability to handle multiple cases was added to the code; this was particularly necessary and important for code verification and validation. A total of 129 test cases were set up to test the BOW code against independent analytical solutions, and ANSYS (a general purpose, finite-element code developed by Swanson Analysis Systems Inc.).

A most complete BOW input file consists of 17 data groups, in which detailed geometries, material properties, boundary conditions, hydraulic drag force, element linear power, drypatches, etc., may be defined. A typical input file may vary from a few lines to thirty lines, depending on the complexity of the problem.

Typical CPU/Turnaround Time and Memory

The CPU (Central Processing Unit) time and memory requirements for running the BOW code are very low. A typical run of the BOW code requires only 0.2 seconds of CPU time, and less than 1 second of turnaround time on our 735-series Hewlett Packard computers at Sheridan Park. Approximately 380K of memory is required for a typical run.

ANALYTICAL VERIFICATIONS AND VALIDATIONS

Closed-Form Analytical Solution and ANSYS

BOW has been verified against closed-form analytical solutions and other independent solutions, such as ANSYS, for a total of 129 cases:

- 48 cases used in verification and validation of lateral deflections,
- 14 cases used in verification and validation of curvature,
- 13 cases used in verification and validation of strains,
- 13 cases used in verification and validation of stresses,
- 6 cases used in verification and validation of contact forces,
- 22 cases used in verification and validation of critical buckling loads, and
- 13 cases used in verification and validation of change in length.

For parameters in the above seven categories, results obtained using the BOW code are in good agreement with analytical and ANSYS solutions. The difference is generally with $\pm 1\%$.

Table 2 compares critical buckling loads predicted by both the BOW and ANSYS codes for a CANDU 6 fuel element supported by different torsional spring constants simulating the endplates. Table 3 compares contact forces for a fuel element with a specified clearance at its midspan, subjected to the axial drag load and concentrated bending moments, between the BOW calculation and closed–form solutions. Table 4 summarizes the verification results of lateral deflections for eleven selected cases.

Figure 5 shows the critical buckling loads of a typical CANDU 6 fuel element at various axial locations. Timoshenko's simplified approximate solution [3] is shown in the same figure for the case when the lateral spring is at the mid–span of the fuel element. Timoshenko's linear assumption gives acceptable results only for the spring constant varying in the neighbourhood of the critical spring constant.

Experimental Data

Two out–of–reactor experiments were performed recently at the Sheridan Park Engineering Laboratory (SPEL) to validate the strength of CANDU 6 unirradiated fuel element and fuel bundle.

In the first experiment, a single CANDU 6 fuel bundle was held horizontally on a load frame at room temperature, while one of its outer elements was pulled radially upwards at the midplane. The radial deflections of the fuel element were measured at two axial locations (midspan and end). Figure 6 shows that there is very good agreement between the measured radial deflections and those calculated using the BOW code. Figure 6 also shows that analytical calculations using hinged supports overpredicted the central deflections by about 40%. This suggests that the endplates exert significant restraints on element deflections. The result is in agreement with the conclusion on endplate restraint in reference [1], based on element vs. bundle deflection of irradiated fuel. Using the averaged slope in the deflection–force curve using measured data, we found that the endplate provides a restraint that is equivalent to 64 Nm/rad of torsional spring constant in the radial coordinate plane. For the same fuel element and endplate dimensions, BOW gives 65 Nm/rad, which is higher than the measured data by only 1%.

In the second experiment, a fuel bundle was compressed vertically between a steel plate and simulated fuelling machine side–stops. The test was conducted at room temperature in air. Strains on various fuel elements and at various axial locations were measured at SPEL. Figure 7 shows the strains measured at four gauge locations on four different fuel elements, and calculated using BOW versus compressive axial force. The trends of the BOW calculation are in good agreement with the measurements. However, due to the non-uniform distribution of the bundle forces, there are some differences in strain magnitude for strains at a particular strain gauge. Figure 8 shows the strain profile along the axial direction calculated using the BOW code. Since the eccentric axial load is applied at one end only, the deflection profile is unsymmetric along the axial direction. At the axial locations close to the endplate, the comparison between the BOW predictions and the experiments is less satisfactory. This is probably caused by the large local plastic deformation of the endplate, and change in eccentricity of the axial load due to the endplate deformation. The calculated strains are in fairly good agreement with the measured strains at the axial locations close to the midspan.

Preliminary checks were also made of BOW predictions vs. two in-reactor experiments. One experiment (WR-928A) was conducted at the Whiteshell Laboratories (Pinawa, Manitoba), and the other (NR) at the Chalk River Laboratories (Chalk River, Ontario). In both experiments, the fuel was irradiated under wet coolant conditions (linear power of 15.1-38.4 kW/m in test WR-928A, and 58-63 kW/m in test NR) for a few months.

The WR-928A fuel bundle was irradiated in organic coolant having a temperature of about 500°C which is much higher than that of normal PHWR (Pressurized Heavy Water Reactor) coolant, hence creep relaxation caused substantial permanent bowing. The NR fuel contained eccentric assembly welds, which exaggerated the bowing caused by the hydraulic drag. Thus the bowing of both of the above fuels is not representative of commercial CANDU fuel. Nevertheless, the exaggerated bows make these irradiations desirable from the perspective of software evaluation.

In the WR-928A experiment, post-irradiation bows of 0.4 to 1.8 mm were measured, for an average of 1.1 mm. For flux-gradient factors in the range 0.032 to 0.7 [2], BOW predicted initial in-reactor bows of 0.56 to 1.2 mm, for an average of 0.9 mm.

In the NR experiment, post-irradiation bows of 0.3 to 1.2 mm were measured [5], for an average of 0.75 mm. BOW predicted initial in-reactor bows of 0.4 to 0.8 mm, for an average of 0.6 mm.

A direct comparison can be made between the above post-irradiation (out-reactor) measurements and BOW-calculated initial deflections, if the thermal recovery (stress relaxation) converts all initial elastic bow to permanent strain, and if the creep in the PHWR adds a negligible amount to the permanent (measured) bow. In addition, there are uncertainties in some input data for BOW calculations; e.g., in the flux-gradient factor, in the curvature-transfer factor, and in the rigidity-enhancement factor. Nevertheless, if the creep is assumed to be insignificant, and if the stress relaxation is assumed to be complete, then the predictions of average bow are within 0.2 mm of the measurements in the experiments. The range of predicted bow is also within the range of measurements.

SUMMARY

This paper has described twelve improvements made to the BOW code since its original release. A total of 129 test cases have been developed and collected in the data base for the BOW code. BOW calculations for all parameters in various categories are generally accurate to within 1% for the tested cases. Predictions of BOW are in excellent agreement with the recent measurements for deflections and endplate torsional spring constants, and are consistent with the two previous post-irradiation measurements taken in experiments performed at Whiteshell Laboratories and Chalk River Laboratories.

ACKNOWLEDGEMENT

The authors wish to express their appreciation to Dr. C. Manu, of AECL, for performing calculations using the ANSYS code in buckling analysis, Mr. D. Dennier, also of AECL, for providing us with the design data in support of the experimental simulation using the BOW code, and Mr. J. MacQuarrie for providing the results of experiments. Funding support from EPDC (Electric Power Development Company Limited, Tokyo, Japan) and COG (CANDU Owners Group) is also gratefully acknowledged.

REFERENCES

(1) TAYAL, M., "Modelling the Bending/Bowing of Composite Beams such as Nuclear Fuel: The BOW Code," *Nuclear Engineering and Design*, **116**, 149–159, 1989.

(2) VEEDER, J., and SCHANKULA, M.H., "Bowing of Pelletized Fuel Elements: Theory and In–Reactor Experiments," *Nuclear Engineering and Design*, **29**, 167–179, 1974.

(3) TIMOSHENKO, S., and GERE, J.M., "Theory of Elastic Stability," McGraw–Hill Book Company, 2nd Ed., 1961.

(4) POPOV, E.P., "Engineering Mechanics of Solids," Prentice–Hall, Inc., 1990, New Jersey, Ch.6.

(5) MEADOWCROFT, R., HYNES, P.E., and TAYAL, M., "Irradiation Behaviour of Prototype 37 - element CANDU Fuel at High Power," *Bulletin of the American Ceramic Society*, **57**(3), p.361, 1978.

TABLE 1
RADIAL AND TANGENTIAL TORSIONAL SPRING CONSTANTS OF A TYPICAL CANDU 6 ENDPLATE

Rigidity Enhancement Factor (REF) and Temperature	Straight Beam Theory		Curved Beam Theory	
	S_r (Nm/Rad)	S_t (Nm/Rad)	S_r(Nm/Rad)	S_t (Nm/Rad)
REF=0.5, T=300C	99.066	97.324	103.29	99.60
REF=0.0, T=300C	77.427	97.324	79.999	99.60
REF=0.0, T=20C	96.397	117.6	99.490	120.37

TABLE 2
CRITICAL BUCKLING LOADS OF A CANDU 6 FUEL ELEMENT WITHOUT LATERAL RESTRAINT USING BOW AND ANSYS

Torsional Spring Constants [kNm / Rad]	Critical Buckling Loads [N]					
	Without Appendages			With Appendages		
	BOW	ANSYS	Difference	BOW	ANSYS	Difference
0.000	1084.4	1092.1	<1%	1084.8	1097.1	<1%
0.081	1658.2	1659.7	<1%	1658.7	1668.1	<1%
0.300	2596.1	2585.6	<1%	2597.0	2603.2	<1%
0.400	2848.7	2840.3	<1%	2849.7	2859.6	<1%
0.500	3040.5	3034.8	<1%	3041.6	3055.7	<1%
1.000	3557.3	3562.3	<1%	3558.7	3585.6	<1%
1.500	3782.8	3787.5	<1%	3784.3	3816.2	<1%
2.000	3907.8	3914.9	<1%	3909.5	3945.1	<1%
3.000	4041.8	4051.1	<1%	4043.6	4082.8	<1%

TABLE 3
COMPARISON OF CONTACT FORCE DUE TO A SINGLE CONTACT AT THE MIDSPAN OF A FUEL ELEMENT

Applied Bending Moment [N.m]	Applied Axial Load [N]	Contact Force [N]		
		Analytical	BOW 1.5	Difference
1.0	1000	16.783	16.909	< 1 %
1.0	2000	68.211	68.313	< 1 %
5.0	100	20.535	20.542	< 1 %
5.0	500	41.069	41.097	< 1 %
5.0	1000	67.291	67.335	< 1 %
5.0	2000	122.194	121.608	< 1 %

TABLE 4
SUMMARY OF VERIFICATION RESULTS FOR SELECTED CASES

Cases	Description of Cases*	Horizontal Direction			Vertical Direction		
		Theory	BOW	Difference	Theory	BOW	Difference
1	200 Nm, 400 Nm 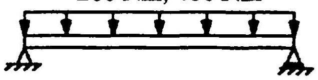	7.016	7.019	< 1%	14.03	14.04	< 1%
2	3 Nm, 4 Nm 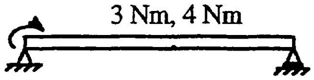	2.074	2.070	< 1%	2.771	2.760	< 1%
3	10 Nm, 6 Nm 	3.367	3.369	< 1%	2.020	2.021	< 1%
4	3 Nm, 4 Nm 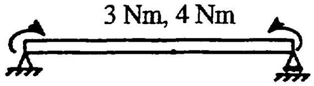	4.040	4.043	< 1%	5.386	5.390	< 1%
5	ΔT=30°C, 60°C 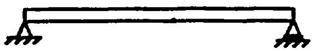	0.328	0.329	< 1%	0.656	0.658	< 1%
6	50 N, 10 N 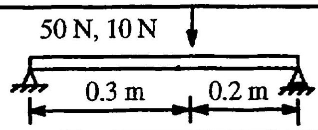 0.3 m 0.2 m	5.300	5.300	< 1%	1.060	1.060	< 1%
7	565 N ΔT = 30°C, 60°C 565 N 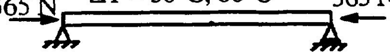	0.873	0.865	< 1%	1.746	1.729	< 1%
8	200 Nm, 400 Nm 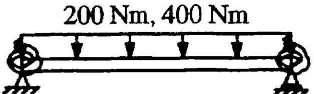 K=200,100 Nm/rad	3.184	3.183	< 1%	8.209	8.211	< 1%
9	565 N 565 N 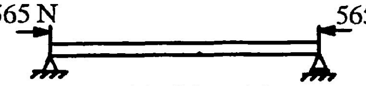 eccentricity 0.5 mm,1.0 mm	1.015	1.006	<1%	2.030	2.012	< 1%
10	565 N 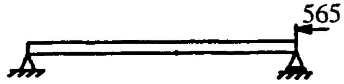 eccentricity 0.5 mm, 1.0 mm	0.5085	0.506	< 1%	1.017	1.011	<1%
11	565 N 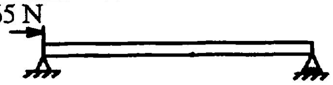 eccentricity 0.5 mm, 1.0 mm	0.5085	0.506	< 1%	1.017	1.011	<1%

* The first load (force, moment, temperature, eccentricity) is applied horizontally; the second load is applied vertically.

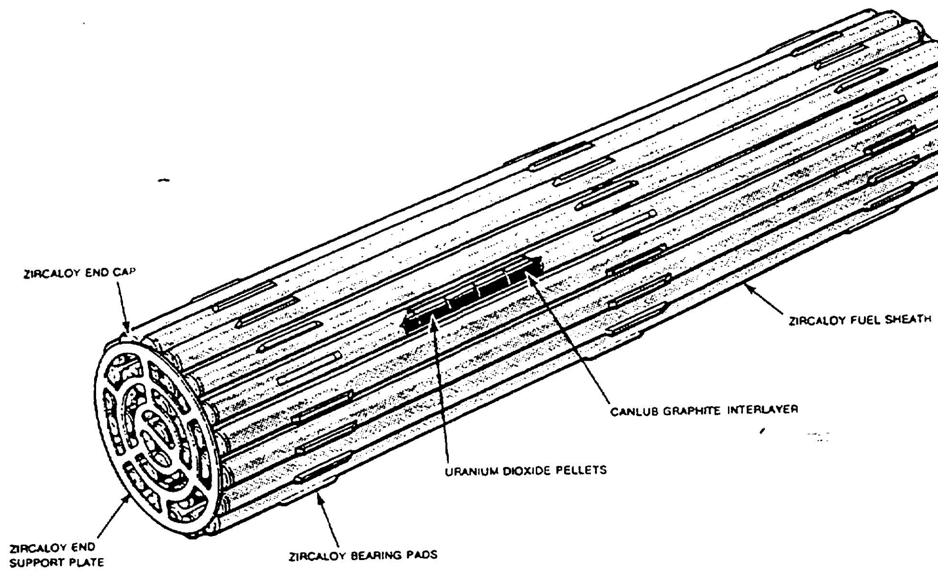

Figure 1 A CANDU 6 FUEL BUNDLE

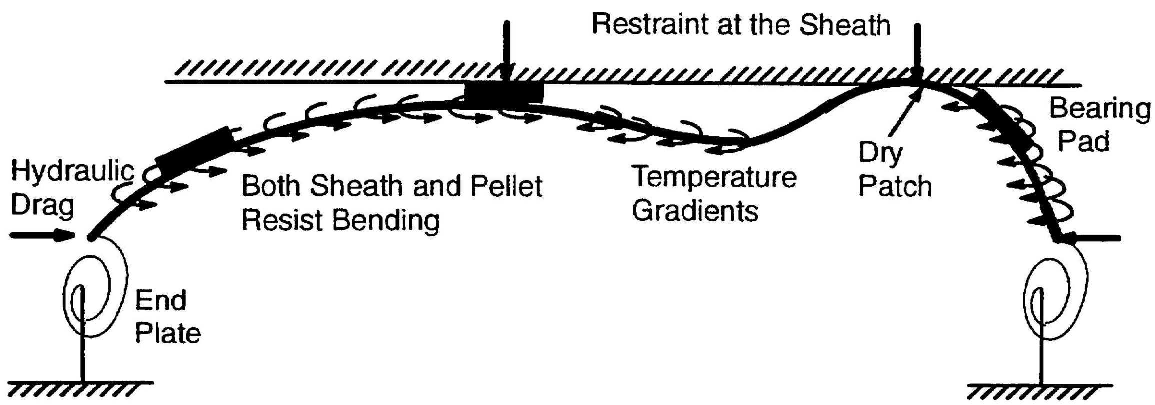

Figure 2 DRIVING FORCES FOR BOWING OF A FUEL ELEMENT

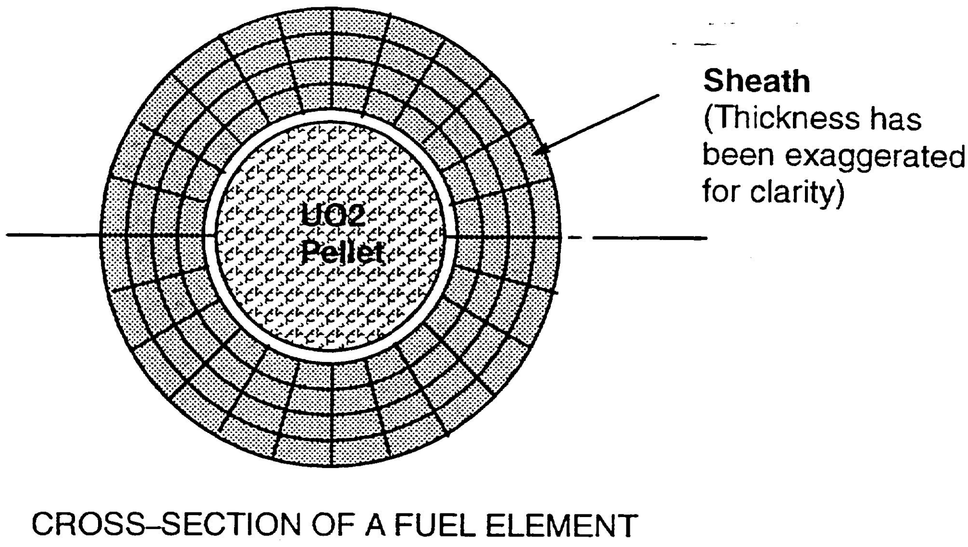

Figure 3 MESH (4×24) USED TO DETERMINE STRAINS AT A CROSS SECTION

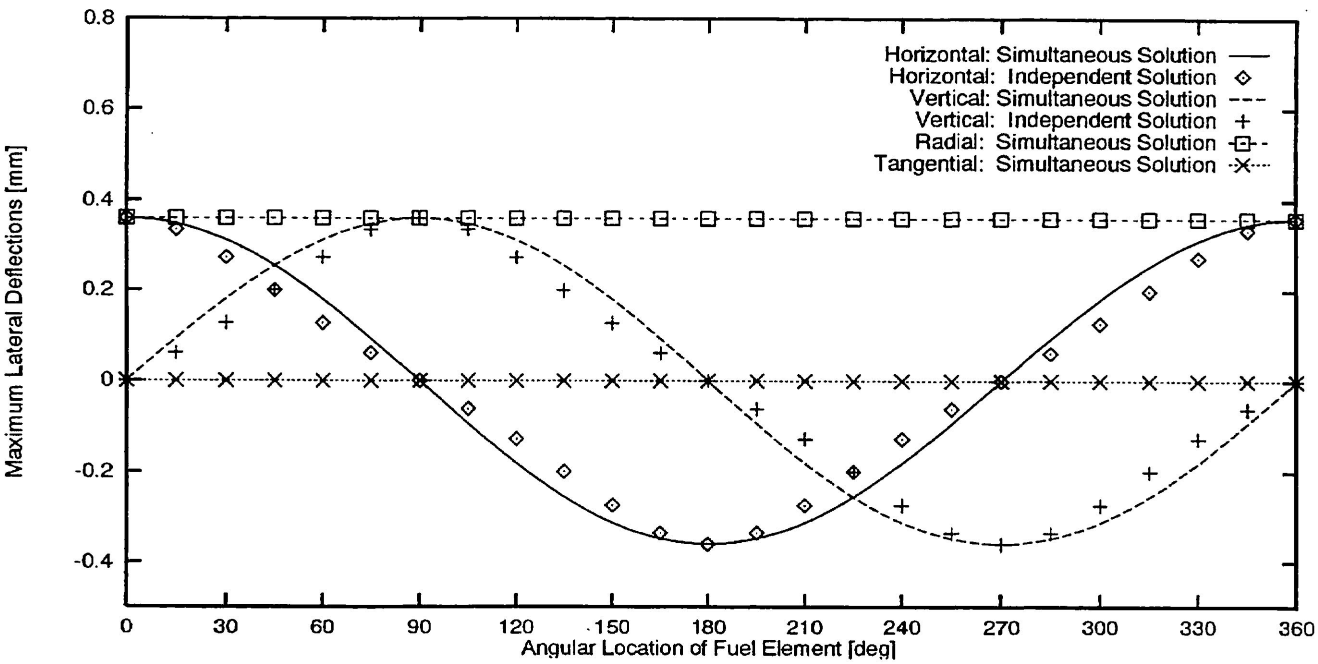

Figure 4 DEFLECTIONS OF A FUEL ELEMENT VS. ANGULAR LOCATIONS WITH REFERENCE TO THE HORIZONTAL AXIS

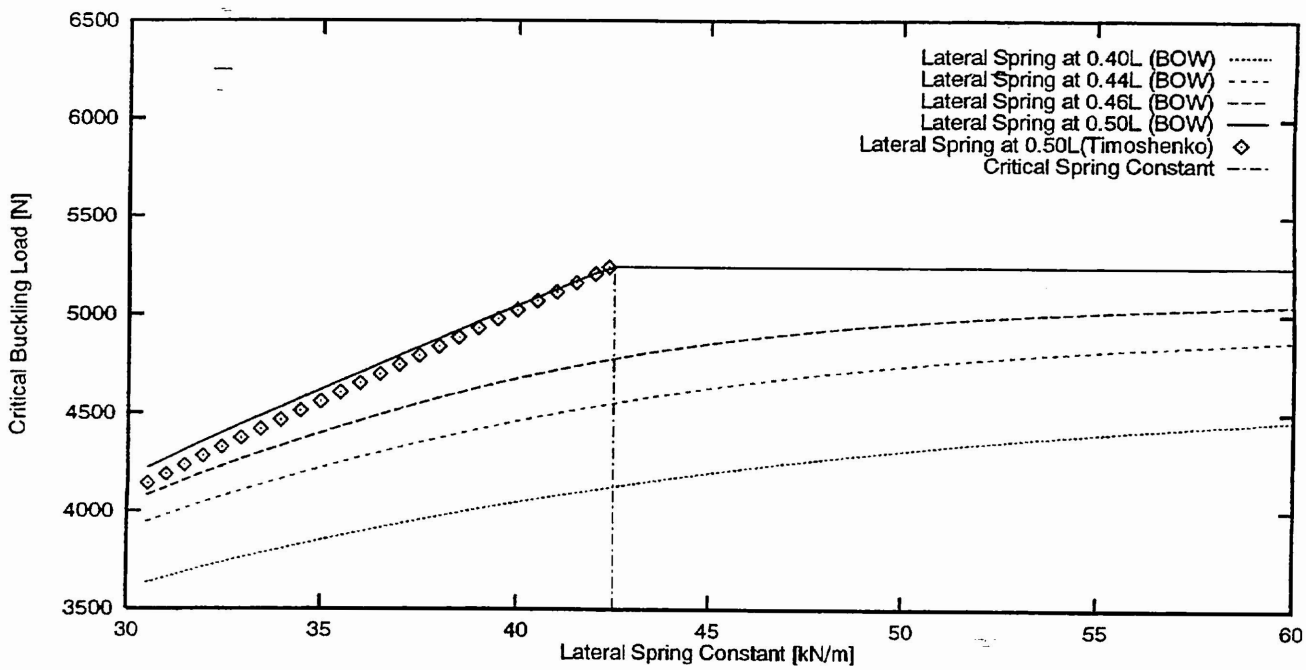

Figure 5 CRITICAL BUCKLING LOADS OF A CANDU 6 FUEL ELEMENT WITH A LATERAL SPRING AT VARIOUS AXIAL LOCATIONS

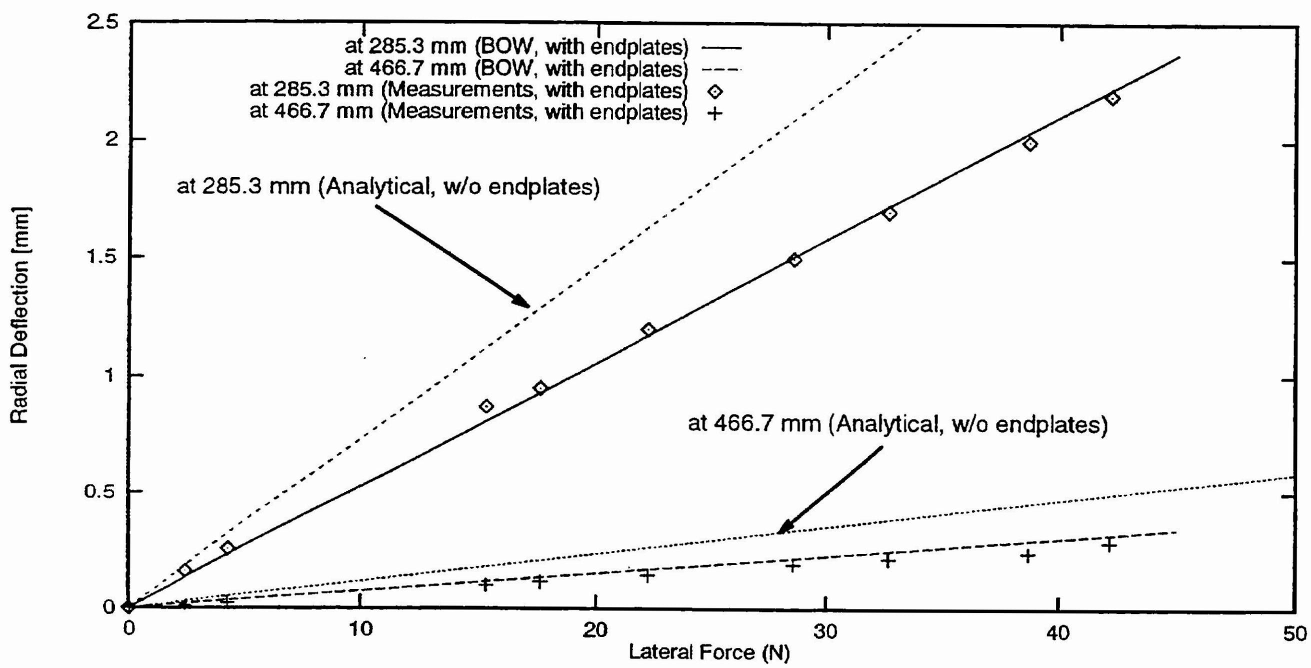

Figure 6 RADIAL DEFLECTIONS OF A FUEL ELEMENT UNDER RADIAL FORCE

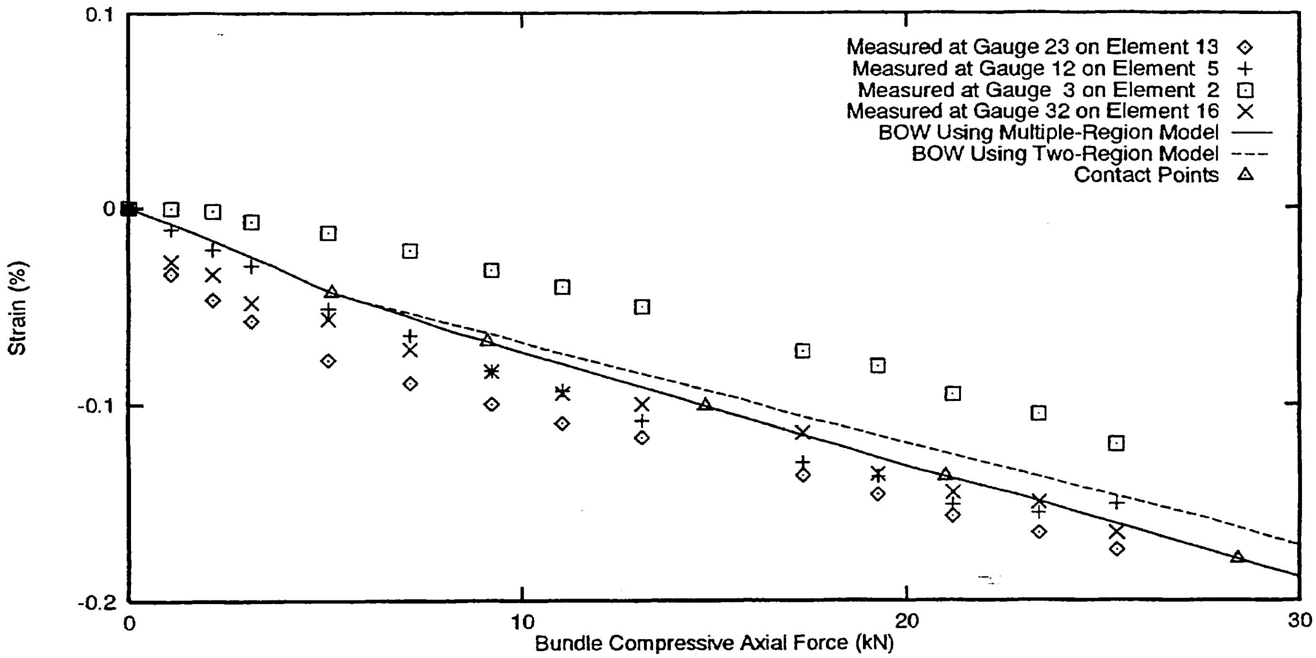

Figure 7: COMPARISON OF BOW CALCULATION WITH MEASUREMENTS OF STRAINS AT RADIAL GAUGES BELOW THE BEARING PADS

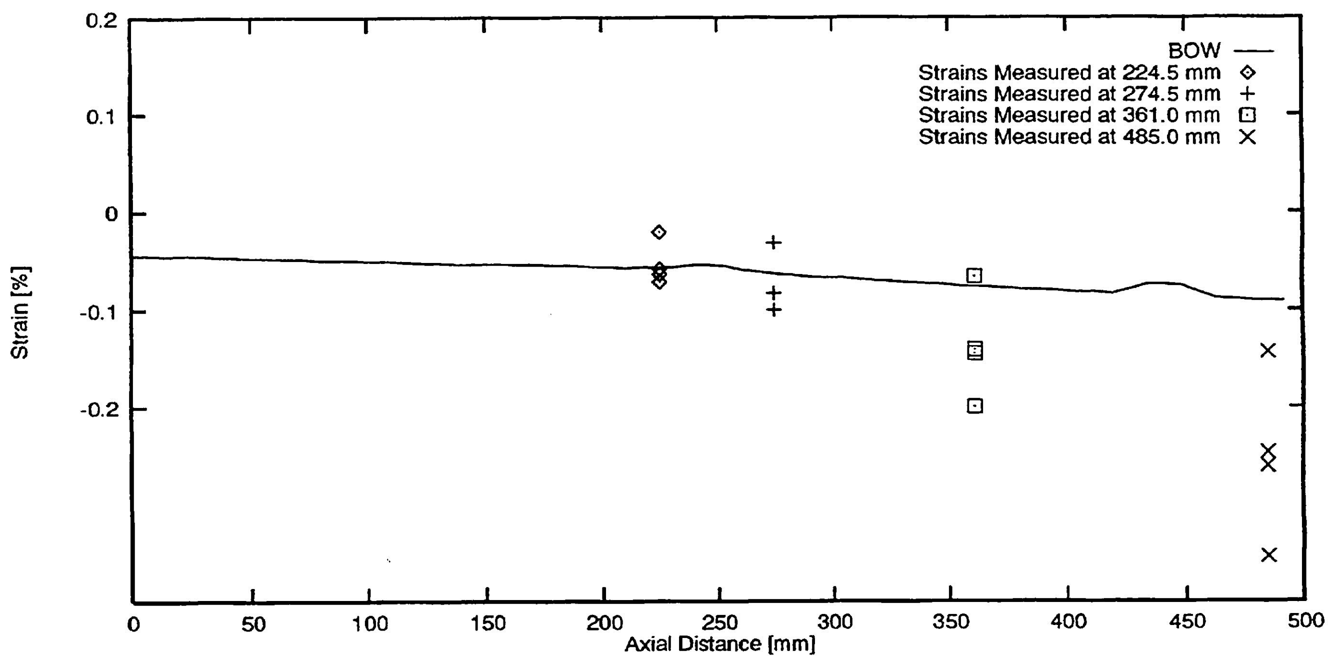

Figure 8: STRAIN PROFILE: MEASUREMENT VS. BOW CALCULATION